

Molecular Mechanics (MM3) Calculations on Oxygen-Containing Phosphorus (Coordination IV) Compounds

E. L. Stewart, N. Nevins, N. L. Allinger, and J. P. Bowen*

Computational Center for Molecular Structure and Design, Department of Chemistry, University of Georgia, Athens, Georgia 30602

Received May 4, 1998

An MM3 force field has been developed for small oxygen-containing phosphorus (coordination IV) compounds. Experimental electron and neutron diffraction, X-ray, and infrared spectral data were utilized in parametrization when available. Results from previous ab initio calculations at both the restricted Hartree–Fock (RHF) and second-order Møller–Plesset (MP2) levels of theory with the standard 6-31G** basis set supplemented missing structural data, rotational profiles, and vibrational frequencies. Negative hyperconjugation (the anomeric effect) affects the structures and energies of the molecules under study which contain one or more sp³-hybridized oxygen atoms. Natural bond order (NBO) analysis was helpful in identifying the key orbital interactions involved in this effect.

Introduction

An understanding of oxygen-containing phosphorus compounds is vital for studying the numerous biological molecules that occur in living systems. Examples of phosphate-containing molecules include simple nucleotides, which join together via phosphodiester linkages to form RNA and DNA, as well as lipids and carbohydrates that contain phosphate functional groups. These phosphate moieties are involved in energy transfer processes in molecules such as ADP and ATP. To mimic certain biological components, many pharmaceutical agents, such as nucleotide analogues used in the treatment of various cancers, contain phosphate groups. Their inclusion in the well-parametrized MM3 force field would provide insight into the structure and conformation of such oxygen-containing phosphate compounds.

The MM3 molecular mechanics force field,¹ one of the more successful force fields in predicting experimental results, has been extended in this work to include compounds containing a coordination IV phosphorus double-bonded to an oxygen and single-bonded to one to three –OR coordinating groups, where R = H or CH₃. Relatively sparse or inaccurate experimental structural data exist for molecules involving this type of phosphorus (see Molecular Mechanics Treatment: Bond Lengths and Angles section). To obtain further structural data, phosphinic, phosphonic, and phosphoric acids and the related esters have been studied by ab initio methods.² MM3 parameters shown in Tables 1–3 have been obtained using these ab initio results in conjunction with the available experimental data. In addition to the new atom type for P(IV), a new atom type for an O_{sp}³ attached to P(IV) was needed to accurately reproduce the data. The dipole moments for this type of oxygen attached to carbon and hydrogen are quite different from the values corresponding to the regular O_{sp}³ atom type 6. In addition, the C–O and O–H stretching frequencies are improved with

Table 1. MM3 Torsion-Related Parameters for Phosphates^a

torsion				V ₁ ^b	V ₂	V ₃
1	1	153	1	0.000	0.000	0.000
1	1	153	5	0.000	0.000	0.000
1	1	153	7	0.000	0.000	0.270
1	1	153	159	0.000	0.000	0.270
5	1	153	1	0.000	0.000	0.100
5	1	153	159	0.000	0.000	0.100
5	1	153	7	0.000	0.000	0.500
1	1	159	153	0.000	0.000	0.000
5	1	159	153	0.000	0.000	0.300
1	159	153	1	1.227	0.432	1.005
1	159	153	5	1.135	0.685	0.806
1	159	153	159	0.207	–0.300	0.974
1	159	153	7	0.000	0.000	0.000
21	159	153	1	2.011	–0.205	0.240
21	159	153	5	1.500	0.200	0.000
21	159	153	159	0.828	0.112	0.280
21	159	153	7	0.000	0.000	0.000
Torsion–Stretch						
	159	153		0.0	0.0	0.4

^a Atom types involved for this set are 1 (C_{sp}³), 5 (H), 159 (O_{sp}³ attached to P(IV)), 7 (O_{sp}² attached to P(IV)), 21 (H attached to O_{sp}³), and 153 (P(IV)). ^b V₁, V₂, and V₃ are expressed in kcal/mol.

addition of the new atom type. The MM3 atom types for P(IV) and O_{sp}³ attached to P(IV) are 153 and 159, respectively.

These parameters were chosen to reproduce the geometries, rotational barriers, vibrational frequencies, and dipole moments of the nine compounds shown in Figure 1, which include phosphine oxide (1), hypophosphorous acid (2), phosphorous acid (3), phosphoric acid (4), dimethylphosphinic acid (5), dimethylphosphonate (6), methyl dimethylphosphinate (7), trimethylphosphine oxide (8), and trimethyl phosphate (9). All of these representative compounds except 2 have experimental data available for comparison.

Computational Methods

Ab Initio. Geometries, rotational barriers, and vibrational frequencies determined from ab initio calculations carried out at the restricted Hartree–Fock (RHF) level³ using the 6-31G**

(1) Allinger, N. L.; Yuh, Y. H.; Lii, J.-H. *J. Am. Chem. Soc.* **1989**, *111*, 8551.

(2) Stewart, E. L.; Nevins, N.; Allinger, N. L.; Bowen, J. P. *J. Org. Chem.* **1997**, *62*, 5198–5207.

Table 2. MM3 Stretch-Related Parameters for Phosphates^{a,b}

bond stretch ^c		K_s	l_0	μ
1	153 ^d	3.30	1.805	0.67
5	153 ^d	3.28	1.398	0.22
159	153 ^{b,d}	5.70	1.600	-0.58
7	153 ^{b,d}	8.90	1.487	-3.40
1	159	4.40	1.424	1.75
159	21	7.78	0.947	-1.57

^a Atom types involved for this set are 1 (C_{sp}³), 5 (H), 159 (O_{sp}³ attached to P(IV)), 7 (O_{sp}² attached to P(IV)), 21 (H attached to O_{sp}³), and 153 (P(IV)). ^b Electronegativity corrections are applied to the following bonds when type 159 is attached to type 153: 1-153: -0.011 Å; 5-153: -0.011 Å; 153-159: -0.015 Å; 153-7: -0.016 Å; a correction of -0.0028 Å is applied to a type 1-5 bond when a type 159 atom is attached to type 1; a correction of -0.003 Å is applied to a type 7-153 bond when a type 5 atom is attached to type 153. ^c Units for K_s , l_0 , and μ are mdyne/Å, Å, and debye (D), respectively. ^d Bohlmann (trans-lone-pair) corrections are applied to the following bonds for each sp³ oxygen (type 159) attached to phosphorus (type 153): BHV1 = BHV2 = 0.004 for 7-153; BHV1 = BHV2 = 0.006 for 159-153 (see eq 2).

Table 3. MM3 Bending-Related Parameters for Phosphates^a

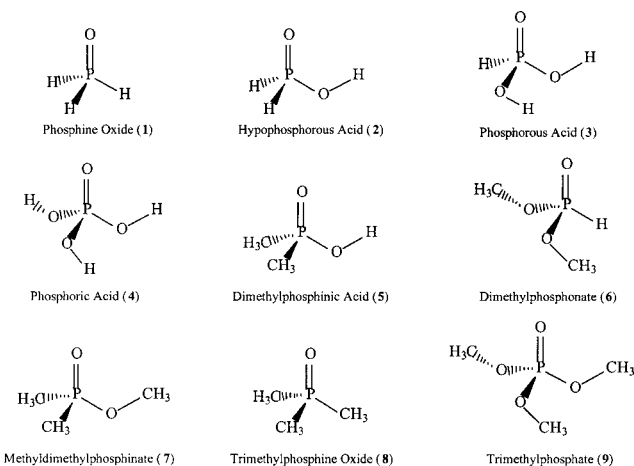
bond angle ^b			K_b	θ_0	type ^c
1	1	153	0.50	109.5	
5	1	153	0.52	109.6	
1	1	159	0.83	109.5	
5	1	159	0.92	108.7	3
1	153	1	0.40	109.2	
1	153	5	0.50	105.5	
1	153	7	0.80	117.5	
1	153	159	0.55	104.7	
5	153	5	0.42	104.5	
5	153	7	0.83	116.7	1
5	153	7	0.83	116.4	2
5	153	7	0.83	119.3	3
5	153	159	0.70	102.0	
159	153	7	1.18	116.2	1
159	153	7	1.18	115.4	2
159	153	7	1.18	116.8	3
159	153	159	0.90	103.5	1
159	153	159	0.90	103.8	2
1	159	153	0.90	118.8	
21	159	153	0.38	112.0	

Stretch-Bend ^d		K_{sb}
type		
X-P-Y		0.10
X-P-H		0.10

^a Atom types involved for this set are 1 (C_{sp}³), 5 (H), 159 (O_{sp}³ attached to P(IV)), 7 (O_{sp}² attached to P(IV)), 21 (H attached to O_{sp}³), and 153 (P(IV)). ^b Units for K_b and θ_0 are mdyne Å/rad² and deg, respectively. ^c Types 1, 2, and 3 apply when the central atom is substituted, respectively, as -CR₂-, -CHR-, and -CH₂-, apart from the atoms that define the angle. ^d Stretch-bend terms (where phosphorus is the central atom, and X and Y are non-hydrogen atoms).

basis set complemented the experimental results and provided a more complete set of data for parametrization.² Calculations at the Møller-Plesset (MP2) level⁴ with the 6-31G** basis set⁵⁻⁹ were performed on some of the smaller structures to determine the effect of electron correlation. The RHF/6-31G**

- (3) Roothaan, C. C. J. *Rev. Mod. Phys.* **1951**, *23*, 69.
 (4) Møller, C.; Plesset, M. S. *Phys. Rev.* **1934**, *46*, 618.
 (5) Ditchfield, R.; Hehre, W. J.; Pople, J. A. *J. Chem. Phys.* **1971**, *54*, 724.
 (6) Hariharan, P. C.; Pople, J. A. *Theor. Chim. Acta* **1973**, *28*, 213.
 (7) Hehre, W. J.; Ditchfield, R.; Pople, J. A. *J. Chem. Phys.* **1972**, *56*, 2257.

**Figure 1.** Small oxygen-containing phosphorus(IV) compounds involved in the force field parametrization.

results were chosen for parametrization because the differences between these RHF and MP2 calculations were small, a full set of MP2 calculations would have been resource intensive, and consistency among the ab initio results was desired. Gaussian 92¹⁰ and Gaussian 94¹¹ were used to carry out all ab initio calculations.

It has been shown that RHF bond lengths can be scaled to existing experimental r_g ones and that these scaling factors can be used to correct the bond lengths of compounds where no experimental data are available.^{12,13} This scaling procedure was used to obtain bond lengths from which the natural bond length parameters for the phosphates were to be determined. Also, RHF vibrational frequencies have been shown to be calculated systematically too large by approximately 10%.¹⁴ Thus, frequencies were scaled and used for parametrization when experimental data was either not available or ambiguous.

MM3(96). MM3(96) calculations were carried out on IBM RS/6000-540 and SGI Indigo2 workstations, with the RHF/6-31G** optimized structures as the starting geometries. Two in-house programs were used to develop the parameters. The program MPMSR (multiparameter multistep relaxation) assisted in fitting the bond lengths, angles, and vibrational frequencies.¹⁵ Although MPMSR gave good starting parameters, adjustments by inspection were still necessary due to the coupling of vibrational modes of some molecules and the nonorthogonality of the parameters. The second program TORSMAST searches for the MM3 torsional terms V_1 , V_2 , and V_3 (see eq 1) which, to within some error limit, reproduce a given rotational profile.¹⁶

- (8) Hariharan, P. C.; Pople, J. A. *Mol. Phys.* **1974**, *27*, 209.
 (9) Gordon, M. S. *Chem. Phys. Lett.* **1980**, *76*, 163.
 (10) Frisch, M. J.; Trucks, G. W.; Head-Gordon, M.; Gill, P. M. W.; Wong, M. W.; Foresman, J. B.; Johnson, B. G.; Schlegel, H. B.; Robb, M. A.; Replogle, E. S.; Gomperts, R.; Andres, J. L.; Raghavachari, K.; Binkley, J. S.; Gonzalez, C.; Martin, R. L.; Fox, D. J.; Defrees, D. J.; Baker, J.; Stewart, J. J. P.; Pople, J. A. *Gaussian 92, Revision B*; Gaussian, Inc.: Pittsburgh, PA, 1992.
 (11) Frisch, M. J.; Trucks, G. W.; Schlegel, H. B.; Gill, P. M. W.; Johnson, B. G.; Robb, M. A.; Cheeseman, J. R.; Keith, T.; Petersson, G. A.; Montgomery, J. A.; Raghavachari, K.; Al-Laham, M. A.; Zakrzewski, V. G.; Ortiz, J. V.; Foresman, J. B.; Cioslowski, J.; Stefanov, B. B.; Nanayakkara, A.; Challacombe, M.; Peng, C. Y.; Ayala, P. Y.; Chen, W.; Wong, M. W.; Andres, J. L.; Replogle, E. S.; Gomperts, R.; Martin, R. L.; Fox, D. J.; Binkley, J. S.; Defrees, D. J.; Baker, J.; Stewart, J. P.; Head-Gordon, M.; Gonzalez, C.; Pople, J. A. *Gaussian 94, Revision B.1*; Gaussian, Inc.: Pittsburgh, PA, 1995.
 (12) McGaughey, G. B.; Stewart, E. L.; Bowen, J. P. *J. Comput. Chem.* **1995**, *16*, 1250-1260.
 (13) Ma, B.; Lii, J.-H.; Schaefer, H. L. I.; Allinger, N. L. *J. Phys. Chem.* **1996**, *100*, 8763-8769.
 (14) Grev, R. S.; Janssen, C.; Schaefer, H. F. I. *J. Chem. Phys.* **1991**, *95*, 5128.
 (15) Liang, G. Y.; Fox, P. C.; Bowen, J. P. *J. Comput. Chem.* **1996**, *17*, 940.

$$E_{\text{tors}} = \frac{1}{2} V_1(1 + \cos \omega) + \frac{1}{2} V_2(1 - \cos 2\omega) + \frac{1}{2} V_3(1 + \cos 3\omega) \quad (1)$$

Natural Bond Order (NBO) Analysis. NBO analyses were performed in Gaussian 94¹¹ at the RHF/6-31G*, RHF/D95*,¹⁷ and RHF/cc-pVDZ levels.^{18–20} Hyperconjugative energies were determined using the NBO deletion procedure.^{21–24} Total SCF, Lewis (covalent interactions only), and deletion (the energy difference between the total SCF energy and the energy calculated after elements corresponding to unfilled orbitals are deleted from the Fock matrix) energies are designated E_{tot} , E_{Lew} , and E_{del} . Thus, energy corresponding to delocalization, as represented by E_{del} , can be assessed. For acyclic phosphates, an energy lowering due to hyperconjugation is observed when the C–O–P(=O)–R (R = H, CH₃, OH, or OCH₃) torsion is in the gauche conformation. For cyclic phosphates, this energy lowering is observed in the axial conformation of the same torsion. This phenomenon is another example of “negative hyperconjugation” which is sometimes referred to as the “generalized anomeric effect”.^{25–27} Negative hyperconjugation can be measured and attributed to specific orbital interactions. For this class of molecules, orbitals corresponding to the sp³ oxygen lone pairs attached to phosphorus donate into antibonding orbitals ($\sigma^*_{\text{P-R}}$) of P=O, P–O, P–C, and P–H bonds.

Molecular Mechanics Treatment

Bond Lengths and Angles. For this class of compounds, ab initio calculations result in bond lengths that are systematically shorter than the same bonds measured by electron diffraction. The short bond lengths from RHF calculations may be attributed to the lack of correlation and basis set truncation, as well as to the fact that the RHF values are r_e , whereas electron diffraction and MM3 determines r_g values. Most of these errors can be reduced by appropriate scaling.⁴ For instance, the electron diffraction P=O and P–O bond lengths of trimethyl phosphate are 0.024 and 0.008 Å longer, respectively, than the RHF determined ones. The electron diffraction P=O bond length of trimethylphosphine oxide is 0.004 Å longer than the ab initio bond length, which is lower than the trimethyl phosphate case. Thus, all RHF P=O and P–O r_e bond lengths have been scaled by an average value of +0.014 and +0.008 Å, respectively, to give r_g bond lengths. The P–H and P–C bond lengths were determined by averaging the bond lengths of RHF/6-31G** and MP2/6-31G** results for each calculated compound. The X-ray and neutron diffraction bond lengths for P=O and P–O bonds are longer and shorter, respectively, than those determined by gas-phase electron diffraction measurements and ab initio calculations. Unfortunately, bond

lengths determined by X-ray and neutron diffraction studies are influenced by crystal packing forces and other interactions and cannot reliably be used in the parameterization of MM3 (r_g) bond lengths. Experimental, adjusted RHF/6-31G**, and MM3 results are presented in Table 4. The RHF/6-31G** results for bond angles were used with no scaling.

Cross Terms and Corrections. Only a few cross terms are permitted in MM3. The set of equations that comprise MM3 has been established for a long time and new equations (cross terms) cannot be added—otherwise previously established parameters would need to be modified, potentially causing differing results from earlier to later versions of the program. However, since the definition of MM3, it has been discovered that additional cross terms would indeed improve MM3 calculations in certain cases. Many of these terms are now included in MM4. As an example, a torsion–bend term is a key cross term that would allow angle and energetic consequences of the anomeric effect to be reproduced in the compounds considered here. This term is not available in MM3 but is in MM4.

Calculating bond lengths with molecular mechanics for phosphates is a challenge, since competing interactions must be deconvoluted. Torsion–stretch, electronegativity, and trans lone pair effect corrections are all required. The P–O bond lengths are relatively longer in molecules with eclipsed O=P–O–R (where R is H or CH₃) dihedral angles compared to those with gauche angles. Thus, a V_3 dependent torsion–stretch term (0.40 mdyne/Å) was included in the force field to reproduce this P–O bond lengthening.

It was also noticed that P=O, P–O, P–C, and P–H bonds were systematically shortened as more sp³ oxygens (atom type 159) were attached to phosphorus. Thus electronegativity corrections are employed for these four bonds when O (atom type 159) was attached to P (atom type 153). The electronegativity effect causes reductions in bond length; in general, the more electronegative the atom, the larger the reduction in bond length.²⁸

The terms “anomeric effect”, “negative hyperconjugation”, “trans lone pair effect”, and “Bohlmann effect” can all be used to describe bond lengthening as a result of donation of lone-pair electrons to an antibonding orbital ($n_{\text{lp}} \rightarrow \sigma^*$ or $n_{\text{lp}} \rightarrow \pi^*$). This effect occurs when an atom with lone-pair electrons (e.g. O, N, S, or halogen) is bonded to a less electronegative atom (C, Si, P) and has been observed experimentally and theoretically.^{21,25–27,29,30} In this study, it was observed that P=O, P–O, P–C, and P–H bonds lengthen when one or more sp³ oxygens is/are attached to phosphorus such that the lone pairs are oriented trans (antiperiplanar) to these bonds. In Table 5, RHF/6-31G* results for axial and equatorial 2-methyl-1,3,2-dioxaphosphinane 2-oxide (X = O) and 1-methylphosphinane 1-oxide (X = CH₂) illustrate the electronegativity and anomeric effect/trans lone pair effect phenomena (also see Figure 2). Both P=O and P–CH₃ bond lengths are reduced by about 0.03 Å due to interactions with sp³ oxygens attached to phosphorus. The trans lone pair effect is evident in the shortening of both these bonds as well. For the axial conformer, where oxygen lone

(16) Liang, G. Y.; Fox, P. C.; Bowen, J. P. *J. Comput. Chem.* **1996**, *17*, 940–953.

(17) Dunning, J. T. H. In *Methods of Electronic Structure Theory*; Schaefer, H. F. I., Ed.; Plenum Press: New York, 1977; Vol. 3, pp 1–28.

(18) Woon, D. E.; Dunning, T. H., Jr. *J. Chem. Phys.* **1993**, *98*, 1358.

(19) Kendall, R. A.; Dunning, T. H., Jr.; Harrison, R. J. *J. Chem. Phys.* **1992**, *96*, 6796.

(20) Dunning, T. H., Jr. *J. Chem. Phys.* **1989**, *90*, 1007.

(21) Tyrell, J.; Weinstock, R. B.; Weinhold, F. *Int. J. Quantum Chem.* **1981**, *19*, 781.

(22) Reed, A. E.; Curtiss, L. A.; Weinhold, F. *Chem. Rev.* **1988**, *88*, 899.

(23) Curtiss, L. A.; Pochatko, D. J.; Reed, A. E.; Weinhold, F. *J. Chem. Phys.* **1983**, *82*, 2679.

(24) Carpenter, J. E. *J. Mol. Struct. (THEOCHEM)* **1988**, *169*, 41.

(25) Kirby, A. J. *The Anomeric Effect and Related Stereoelectronic Effects at Oxygen*; Springer-Verlag: Berlin, 1983.

(26) Reed, A. E.; Schleyer, P. V. R. *J. Am. Chem. Soc.* **1987**, *109*, 7362–7373.

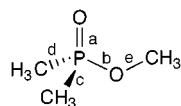
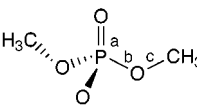
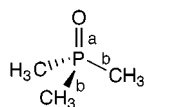
(27) Salzner, U.; Schleyer, P. V. R. *J. Am. Chem. Soc.* **1993**, *115*, 10231–10236.

(28) Allinger, N. L.; Imam, M. R.; Frierson, M. R.; Yuh, Y. H.; Schafer, L. In *Mathematics and Computational Concepts in Chemistry*; Trinajstić, N., Ed.; E. Horwood, Ltd.: London, 1986; p 8.

Table 4. Phosphate Geometries

structure	label ^a	expt ^b	RHF/ 6-31G**	MM3	Δ	structure	label ^a	expt ^b	RHF/ 6-31G**	MM3	Δ	
 phosphine oxide (1)	a		1.479	1.482	0.003	 phosphoric acid (4b)	a	1.460	1.460	0.000		
	b		1.399	1.399	0.000		b		1.592	1.592	0.000	
	rms				0.002		c		1.580	1.582	0.002	
							d		1.592	1.592	0.000	
							e, g		0.946	0.947	0.001	
	ab		116.9	116.9	0.0	f		0.946	0.946	0.000		
	bc		101.1	101.1	0.0	rms				0.001		
	rms				0.0							
 hypophosphorous acid (2)	a		1.471	1.471	0.000	ab		115.2	114.8	-0.4		
	b		1.604	1.611	0.007	ac		114.8	115.8	1.0		
	c, d		1.391	1.390	-0.001	ad		115.2	114.8	-0.4		
	e		0.947	0.947	0.000	bc		103.7	103.1	-0.6		
	rms				0.004	bd		102.6	103.6	1.0		
		ab		115.4	115.6	0.2	cd		103.7	103.1	-0.6	
		ac		115.9	116.2	0.3	be		112.8	113.2	-0.4	
		bc		102.0	101.6	-0.4	cf		115.9	114.0	-1.9	
		be		113.1	112.6	-0.5	dg		112.8	113.2	0.4	
		cd		103.5	103.5	0.0	rms				0.9	
		rms				0.3	abe		2.2	17.1	14.9	
		abe		0.0	0.0	0.0	acf		180.0	180.0	0.0	
							adg		-2.2	-17.1	-14.9	
							rms				12.4	
	 phosphorous acid (3)	a	1.47	1.467	1.465	-0.002	 dimethylphosphinate (5)	a	1.495 (4)	1.479	1.475	-0.004
b, c		1.54	1.594	1.599	0.005	b		1.559 (4)	1.617	1.616	-0.001	
d			1.381	1.383	0.002	c		1.781 (6)	1.805	1.805	0.000	
e, f			0.947	0.947	0.000	d		1.776 (6)	1.805	1.805	0.000	
rms					0.003	e			0.946	0.947	0.001	
		ab	113	114.3	114.6	0.3		rms				0.002
		ac	116	114.3	114.3	0.3		ab	112.7 (2)	112.9	113.7	0.8
		bc	102	105.3	104.4	-0.9		ac	111.0 (2)	114.9	115.3	0.4
		ad		118.2	117.4	-0.8		ad	112.1 (3)	114.9	115.3	0.4
		cd		101.4	102.0	-0.6		bc	108.8 (2)	103.1	102.6	-0.5
		bd		101.5	102.0	-0.5		cd	107.3 (3)	106.6	105.8	-0.8
		ce		113.2	113.3	0.1		bd	104.6 (3)	103.1	102.6	-0.5
		rms				0.6		be		111.6	111.9	0.3
		ace		-11.6	-10.8	0.8		rms				0.6
		bce		114.7	115.3	0.6		abe	0	0.0	0.0	0.0
	rms				0.7							
 phosphoric acid (4a)	a	1.502	1.464	1.468	0.004	 dimethyl phosphonate (6)	a		1.469	1.470	0.001	
	b, d	1.562	1.584	1.578	-0.006		b		1.384	1.385	0.001	
	c	1.556	1.584	1.578	-0.006		c		1.582	1.583	0.001	
	e	0.965	0.946	0.947	0.001		d		1.594	1.594	0.000	
	f	0.989	0.946	0.947	0.001		e		1.432	1.431	-0.001	
	g	1.001	0.946	0.947	0.001		f		1.432	1.431	-0.001	
	rms				0.004		rms					0.001
		ab	113.3 (3)	115.5	114.9		-0.6	ab		115.7	116.4	0.7
		ac	112.3 (3)	115.5	114.9		-0.6	ac		117.6	115.4	-2.2
		ad	113.2 (3)	115.5	114.9		-0.6	ad		114.1	115.0	0.9
		bc	105.6 (2)	102.8	103.5		0.7	bc		99.9	101.9	2.0
		bd	104.9 (2)	102.8	103.5		0.7	bd		105.0	101.9	-3.1
		cd	107.3 (3)	102.8	103.5		0.7	cd		102.6	104.3	1.8
		be	116.8	113.5	113.9		0.4	ce		121.6	121.1	-0.5
		cf	118.3	113.5	113.9		0.4	df		121.7	121.1	-0.6
	dg	116.3	113.5	113.9	0.4	rms				1.7		
	rms				0.6	adf		29.9	47.6	17.7		
	abe		33.3	48.7	15.4	ace		50.6	52.5	2.0		
	cbe		160.1	174.8	14.7	dce		-75.4	-74.5	0.9		
	dbe		-93.4	-77.5	15.9	cdf		158.1	175.0	16.9		
	rms				15.3	rms				12.3		

Table 4 (Continued)

structure	label ^a	expt ^b	RHF/ 6-31G**	MM3	Δ	structure	label ^a	expt ^b	RHF/ 6-31G**	MM3	Δ
 methyl dimethylphosphinate (7)	a	1.50	1.479	1.478	-0.001	 trimethyl phosphate C ₃ (9a)	a	1.477 (6)	1.467	1.471	0.004
	b	1.56	1.610	1.607	-0.003		b	1.580 (2)	1.580	1.583	0.003
	c	1.78	1.812	1.808	-0.004		c	1.432 (5)	1.433	1.433	0.001
	d	1.78	1.804	1.803	-0.001		rms				0.003
	e	1.43	1.429	1.429	0.000		ab		115.4	115.1	-0.3
	rms				0.002		bb	105.0 (2.9)	102.9	103.3	0.4
	ab	112	114.5	114.5	0.0		bc	118.3 (1.5)	121.0	121.2	0.2
	ac	112	115.5	114.8	-0.7		rms				0.3
	ad	112	113.4	115.2	1.8		abc		44.7	52.8	8.1
	bc	109	104.6	103.1	-1.5		a		1.461	1.465	0.004
	bd		100.8	102.3	1.5		b		1.594	1.594	0.000
	cd	107	106.7	105.4	-1.3		c		1.577	1.585	-0.008
be	118	121.4	121.3	-0.1	d		1.582	1.583	0.001		
rms				1.2	e		1.433	1.433	0.000		
abe		33.4	43.7	10.3	f		1.431	1.434	0.003		
cbe		-87.1	-81.6	5.5	g		1.433	1.432	0.001		
dbe		158.1	169.1	11.0	rms				0.004		
rms				8.0	ab		114.1	114.6	0.5		
 trimethylphosphine oxide (8)	a	1.476 (2)	1.488	1.490	0.002	ac		114.0	115.0	1.0	
	b	1.809 (2)	1.818	1.816	-0.002	ad		117.2	115.0	2.2	
	rms				0.002	bc		105.9	103.7	2.2	
	ab	114.4 (7)	113.8	114.0	0.2	bd		101.7	103.3	1.6	
	bb	104.1 (8)	104.9	104.6	-0.3	be		120.6	121.0	0.4	
	rms				0.3	cd		102.3	103.7	1.4	
						cf		123.6	122.5	-1.1	
						dg		121.0	121.1	0.1	
						rms				1.4	
						abe		35.0	49.7	14.7	
						adg		49.2	51.1	1.9	
						acf		176.3	177.0	0.7	
					rms				8.6		

^a A letter defines the bond length, e.g., the bond length of P=O in phosphine oxide is "a" while two letters define a bond angle, e.g., the bond angle O=P-H in phosphine oxide is "ab", etc. ^b Experimental, RHF, and MM3 bond lengths are r_g values expressed in angstroms. The experimental, RHF, and MM3 bond angles are expressed in degrees.

Table 5. RHF/6-31G* Results for Axial/Equatorial 2-Methyl-1,3,2-dioxaphosphinane 2-Oxide (R = CH₃, X = O) and 1-Methylphosphinane 1-Oxide (R = CH₃, X = CH₂) (See Figure 9)

	2-methyl-1,3,2-dioxaphosphinane 2-oxide			1-methylphosphinane 1-oxide		
	axial ^a	equatorial	diff (ax - eq)	axial	equatorial	diff (ax - eq)
C-X-P=O ^b	±156.8	±70.4		±167.1	±69.3	
P=O ^c	1.447	1.456	-0.009	1.475	1.477	-0.002
X-P=O ^d	113.7	114.6	+0.9	114.3	113.9	+0.8
C-X-P-CH ₃	±77.4	±161.0		±68.0	±164.7	
P-CH ₃	1.804	1.790	+0.014	1.820	1.818	+0.002
X-P-CH ₃	105.4	103.8	+1.6	106.1	106.4	-0.3
C-X	1.418	1.426	-0.008	1.538	1.539	-0.002
C-X-P	123.5	117.1	+6.4	114.6		
X-P	1.594	1.597	-0.003	1.823	1.822	+0.001
X-P-X	103.3	101.1	+2.2			

^a All bond lengths are r_g values in angstroms. All bond angles are in degrees. All torsion angles are in degrees. ^b Represents the torsion angle defined by the atoms C, X, P, and O. ^c Represents the bond length defined by the atoms P and O. ^d Represents the bond angle defined by the atoms X, P, and O.

pairs are antiperiplanar to $\pi^*_{\text{P-CH}_3}$, the P-CH₃ bond is 0.014 Å longer than for the equatorial one. Similarly, in the equatorial conformer, where oxygen lone pairs are antiperiplanar to $\pi^*_{\text{P=O}}$, the P=O bond is 0.009 Å longer than in the axial one.

NBO analysis offers insight into the role played by occupied antibonding orbitals in stabilizing conformations where lone pairs are antiperiplanar to σ and π bonds.

Favorable orbital overlap affords electron donation into antibonding orbitals (delocalization), thereby stabilizing these conformations. This phenomenon, as observed in phosphates, is slightly more complex than that observed in compounds such as dimethoxymethane and pyranose since the delocalization of electrons to the P=O and P-R bonds is dependent on the number of sp³ oxygens attached to the phosphorus.

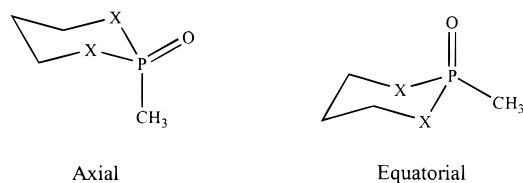


Figure 2. Axial/equatorial 2-methyl-1,3,2-dioxaphosphinane 2-oxide (X = O) (**10**) and 1-methylphosphinane 1-oxide (X = CH₂) (**11**).

Bohlmann Effect. The “Bohlmann band effect” has been described for C–H bonds based on experimentally observed splittings of C–H stretching frequencies in the IR.^{31,32} These splittings have been attributed to C–H bond lengthening as a result of the trans orientation of oxygen lone pairs to the C–H bond. Equation 2 is a general equation that describes the change in bond length as a function of the number of trans lone pairs (Δl_{tp}).³³

$$\Delta l_{\text{tp}} = \text{BHV0} + (1/2)\text{BHV1}(1 + \cos \omega) + (1/2)\text{BHV2}(1 + \cos 2\omega) \quad (2)$$

Currently in MM3, X can be O, N, S, or a halogen and Y can be C, N, or P. BHV0, BHV1, and BHV2 are internal coefficients. The treatment of the Bohlmann Band effect (also called “trans lone pair effect”) in MM3 has been discussed extensively for C–H bonds.³³ The principle is similar for P–X bonds (where X is H, C, O).

Torsion–Bend Cross Term. This term as illustrated in eq 3 accounts for an increase in bond angles such as C–P–O and C–C–P in a gauche conformation as compared to the anti conformation. For a A–B–C–D (ω) torsion, the parameters K_{tb1} , K_{tb2} , and K_{tb3} can increase angles A–B–C ($\Delta\theta_1$) and/or B–C–D ($\Delta\theta_2$) when ω is cis or gauche but has little or no effect in the trans conformation. If a torsion–bend cross term was available for MM3, both the angle increasing and energy lowering characteristics of molecules exhibiting the anomeric effect could be reproduced. Unfortunately, this term is available only in MM4.³⁴

$$E_{\text{tb}} = 2.51124\{[K_{\text{tb1}}(1 + \cos \omega) + K_{\text{tb2}}(1 - \cos 2\omega) + K_{\text{tb3}}(1 + \cos 3\omega)]\Delta\theta_1 + [K_{\text{tb1}}(1 + \cos \omega) + K_{\text{tb2}}(1 - \cos 2\omega) + K_{\text{tb3}}(1 + \cos 3\omega)]\Delta\theta_2\} \quad (3)$$

Rotational Profiles and Optimized Conformers. Rotational profiles calculated by RHF/6-31G** and MM3 are presented in Figures 3–8 for the O=P–O–R (R=H, CH₃) torsions of hypophosphorous acid, phosphorous acid, dimethylphosphinate, methyl dimethylphosphinate, and trimethyl phosphate. At each point along the potentials, the relevant dihedral angle was held constant while the remaining degrees of freedom were optimized. The RHF results guided the MM3 parametrization of the torsional potentials. Some profiles could be

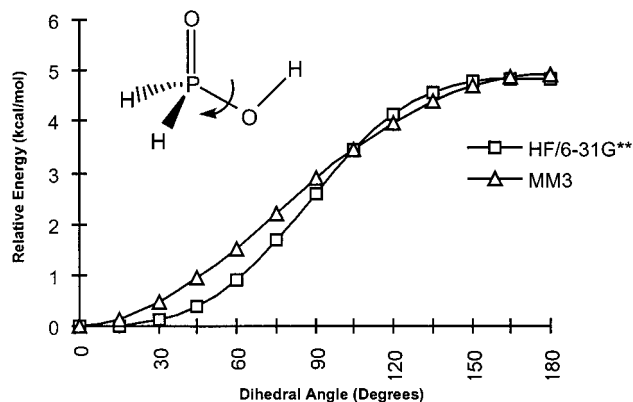


Figure 3. HF/6-31G** and MM3 rotational profiles for the O=P–O–H torsion of hypophosphorous acid.

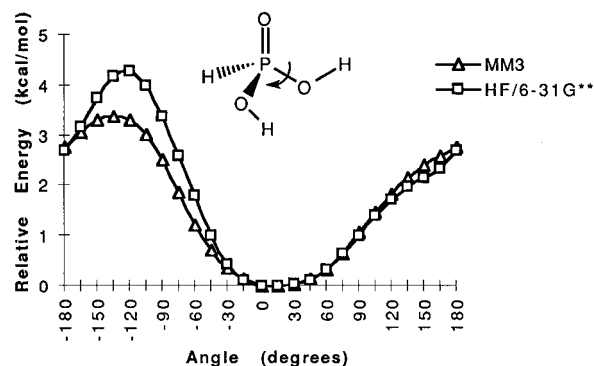


Figure 4. HF/6-31G** and MM3 rotational profiles for the O=P–O–H torsion of phosphorous acid.

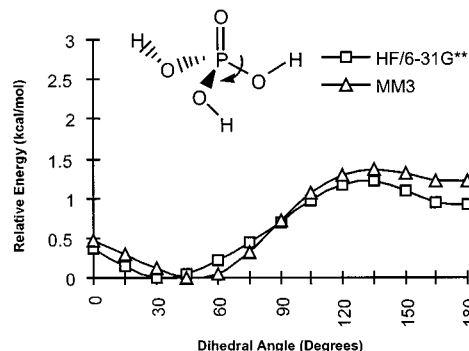


Figure 5. HF/6-31G** and MM3 rotational profiles for the O=P–O–H torsion of phosphoric acid.

fit better if appropriate cross terms were available for MM3. All of the cross terms that are mentioned are available for MM4.³⁴

Dipole Moments. Unfortunately, there are few experimental dipole moments for small phosphate-containing compounds. Many dipole moments reported in the literature are the average dipole moment of all conformers present in the sample. Hence, the RHF dipole moments, which have been scaled by 90% for each of the nine compounds,³⁵ were used for parametrization and comparison with the MM3 dipole moments. The results are reported in Table 6. This scaling seemed reasonable because the RHF calculated P=O and P–O bond lengths are shorter than experiment and caused the calculated

(29) Thatcher, G. R. J. *The Anomeric Effect and Associated Stereoelectronic Effects*; American Chemical Society: Washington, DC, 1992; Vol. 539.

(30) Cramer, C. J. *J. Mol. Struct. (THEOCHEM)* **1996**, *370*, 135–146.

(31) Bohlmann, F. *Angew. Chem.* **1957**, *69*, 641.

(32) Bohlmann, F. *Chem. Ber.* **1958**, *91*, 2157.

(33) Thomas, H. D.; Chen, K.; Allinger, N. L. *J. Am. Chem. Soc.* **1994**, *116*, 5887.

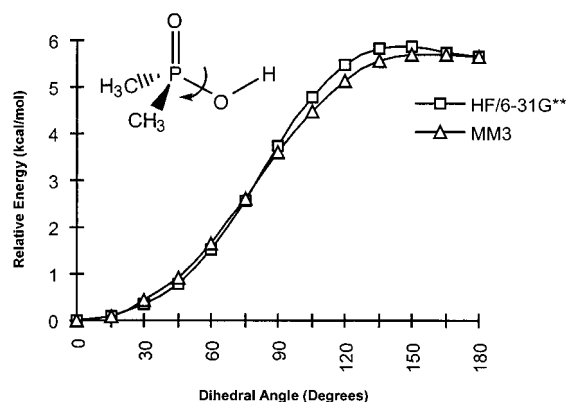
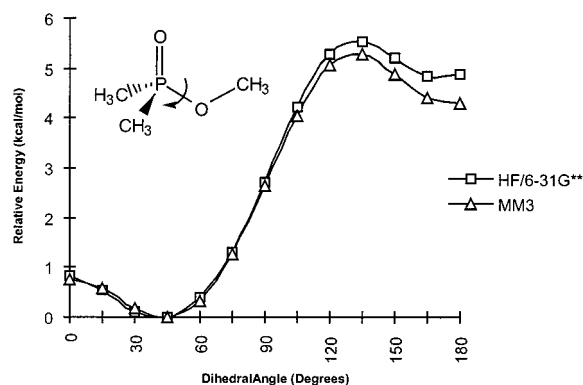
(34) Nevins, N.; Chen, K.; Allinger, N. L. *J. Comput. Chem.* **1996**, *17*, 669–694.

(35) Cornell, W. D.; Cieplak, P.; Bayly, C. I.; Kollman, P. A. *J. Am. Chem. Soc.* **1993**, *115*, 9620.

Table 6. Dipole Moments^a

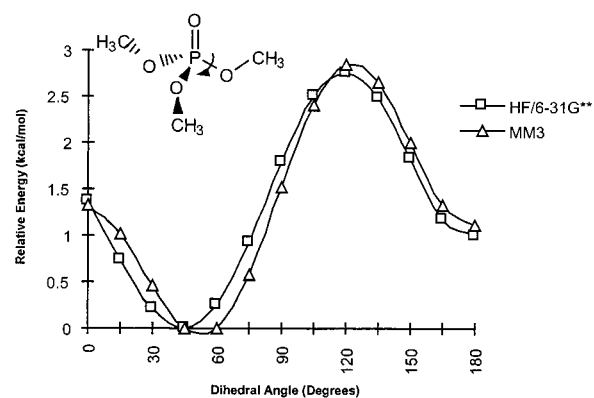
	RHF/6-31G** ^b	MM3/RHF/6-31G** ^c	MM3 ^d	Δ_1^e	Δ_2^f
phosphine oxide	3.769	3.706	3.699	-0.063	-0.070
hypophosphorous acid	2.266	2.349	2.343	0.083	0.077
phosphorous acid	1.279	1.319	1.310	0.040	0.031
phosphoric acid C_1	2.945	2.926	2.748	-0.019	-0.197
phosphoric acid C_3	0.220	0.202	0.893	-0.018	0.673
dimethylphosphinic acid	2.715	2.620	2.641	-0.095	-0.074
dimethylphosphonate	2.215	2.254	2.409	0.039	0.194
methyl dimethylphosphinate	3.025	3.076	3.290	0.051	0.265
trimethylphosphine oxide ^g	4.204	4.210	4.218	0.006	0.014
trimethyl phosphate C_1	3.613	3.540	3.734	-0.073	0.121
trimethyl phosphate C_3	0.908	0.924	1.356	0.016	0.448

^a All dipole moments are expressed in debyes. ^b RHF/6-31G** dipole moment scaled by 0.9. ^c MM3 dipole moments calculated for optimized RHF/6-31G** geometries. ^d MM3 dipole moment for MM3 optimized geometries. ^e Δ_1 is the difference between MM3 (optimized RHF/6-31G** geometries) and optimized RHF/6-31G** dipole moments. ^f Δ_2 is the difference between MM3 (MM3 optimized geometries) and RHF/6-31G** dipole moments. ^g Experimental dipole moments for trimethylphosphine oxide have been determined in various nonpolar solvents and average 4.2 D (see ref 36).

**Figure 6.** HF/6-31G** and MM3 rotational profiles for the O=P-O-H torsion of dimethylphosphinate.**Figure 7.** HF/6-31G** and MM3 rotational profiles for the O=P-O-CH₃ torsion of methyl dimethylphosphinate.

dipole moments to be too large. MM3 dipole moments are reported for both the RHF/6-31G** optimized geometries and the MM3 optimized geometries, since differences in their conformation and geometry influences the dipole moments. Experimental dipole moments for trimethylphosphine oxide have been determined in various nonpolar solvents and average 4.2 D.³⁶ Both phosphoric acid and trimethyl phosphate have a C_1 and C_3 ab initio calculated conformations. As would be expected, the C_3 conformer's dipole moment is much smaller than that of the C_1 . Since calculated dipole moments are mainly determined by the conformations of these compounds,

(36) McClellan, A. L. *Tables of Experimental Dipole Moments*; Raha Enterprises: El Cerrito, CA, 1974; Vol. 2.

**Figure 8.** HF/6-31G** and MM3 rotational profiles for the O=P-O-CH₃ torsion of trimethyl phosphate.

differences in torsion angles between the RHF and MM3 calculated structures result in corresponding dipole moment differences. All reported experimental dipole moments need to be compared to MM3 dipole moments calculated from a Boltzmann-weighted average of conformational energies. The experimental (determined in CCl₄) and Boltzmann averaged MM3 dipole moments for trimethyl phosphate are 3.02 and 2.84 D, respectively, and for dimethylmethyl phosphate are 2.86 and 2.76 D, respectively.

Vibrational Frequencies. Experimental IR spectra are available for four of the nine compounds in Figure 1: phosphine oxide,³⁷ phosphoric acid,³⁸ dimethylphosphonate,³⁹ methyl dimethylphosphinate,⁴⁰ and trimethyl phosphate.⁴¹ The experiments involving the first and fourth compounds were carried out in the gas phase while the remaining were determined in solution. The scaled RHF frequencies of the remaining five compounds for which no experimental data are available were used for comparison to the MM3 calculated frequencies. For methyl dimethylphosphinate and trimethyl phosphate, not all of the experimental IR frequencies could be resolved from their spectra. These missing modes were supplemented with the RHF frequencies. The gas-phase

(37) Whitnall, R.; Andrews, L. *J. Phys. Chem.* **1987**, *91*, 784.

(38) Chapman, A. C.; Thirlwell, L. E. *Spectrochim. Acta* **1964**, *25A*, 47.

(39) Nyquist, R. A. *Spectrochim. Acta* **1969**, *25A*, 47.

(40) Odeurs, R. L.; Van der Veken, B. J.; Herman, M. A. *J. Mol. Struct.* **1984**, *17*, 235.

(41) Burkhardt, E. G.; Hohn, E. G.; Goubeau, J. *Z. Anorg. Allg. Chem.* **1978**, *442*, 19.

Table 7. Vibrational Frequency Summary^a

	Δ_{exp}^b	Δ_{RHF}^c
phosphine oxide	18	22
hypophosphorous acid		76
phosphorous acid		53
phosphoric acid		31
dimethylphosphinic acid		27
dimethylphosphonate	50	30
methyl dimethylphosphinate	26	27
trimethylphosphine oxide		31
trimethyl phosphate	31	25
dimethyl methylphosphonate	27	27
rms	32	38

^a All vibrational frequencies in this table are expressed in cm^{-1} .

^b Rms difference between MM3 and experimental IR frequencies.

^c Rms difference between MM3 and RHF/6-31G** frequencies scaled by 0.90.

IR spectrum for dimethyl methylphosphonate was not part of the parametrization data set but was used to validate the MM3 force field. A summary of the vibrational frequency differences between MM3 and experimental/ab initio results is presented in Table 7. The overall rms error for RHF/6-31G** frequencies of the 10 compounds is 38 cm^{-1} ; the rms error for the five compounds with experimental IR data is 34 cm^{-1} and are representative of the accuracy of MM3 calculations. As for the structural data, significant improvements could be implemented if the appropriate cross terms could be included. Experimental (when available), scaled RHF/6-31G**, and MM3 frequencies for each compound in Figure 1 are presented in Tables 8 and 9 and S1–S8 in the Supporting Information.⁴²

Results by Molecule

Phosphine Oxide. Phosphine oxide has no proper torsion angles and thus just one conformation. Only a few parameters are associated with this molecule: those involved with the P=O and P–H bond length and the H–P–H and O=P–H angles. Whitnall and Andrews have assigned the gas-phase IR frequencies of this molecule.³⁷ A comparison between the MM3 and gas-phase frequencies shown in Table 8 finds an rms error of 18 cm^{-1} for six frequencies, a good result for these calculations. The O=P–H and H–P–H bending modes are strongly coupled, and thus the force and natural angle parameters were chosen such that both vibrational frequencies and geometries were reproduced adequately.

Hypophosphorous Acid. No experimental data exist for this molecule. The MM3 results agree with most of the ab initio vibrational frequencies, but several frequencies (see Table 9) significantly deviate from MM3 values, resulting in the largest rms error (76 cm^{-1}) of the phosphate class. The PH_2 scissoring mode is calculated too high ($+47 \text{ cm}^{-1}$), and the PH_2 rocking mode is calculated too low (-162 cm^{-1}). A bend–torsion–bend interaction term could be used to improve these frequencies but is unavailable in MM3. The torsional H–P–O–H frequency is calculated too large ($+183 \text{ cm}^{-1}$); however, attempting to reduce this frequency increases a similar frequency in phosphorous acid, leading to a larger deviation from the ab initio results. Also, this same torsional frequency is calculated only $+39 \text{ cm}^{-1}$ greater than the MP2/6-31G** frequency (scaled by 0.95). The torsional

potential well for O=P–O–H (and H–P–O–H) is very shallow near the minimum (see Figure 3). Thus, the values for dihedral angles and vibrational frequencies associated with these torsions are very sensitive to changes in corresponding torsional parameters. Parameters are selected to best fit geometries, conformational energies, rotational barriers, and vibrational frequencies as a whole. Compromises sometimes must be made so that all data are fit within some margin of error. These compromises had to be made when selecting torsional parameters for many of the dihedrals in the phosphate-containing compounds.

Phosphorous Acid. Two MM3 torsional H–P–O–H modes of this molecule are calculated 101 cm^{-1} lower and 88 cm^{-1} higher than the corresponding RHF frequencies (see Table S1). The O=P–O–H torsion angles and associated vibrational modes are quite sensitive to changes in the torsion parameters and can fluctuate wildly with only small variations in the V_3 term. These drastic changes are due to a shallow torsional potential for this torsion. While RHF predicts a minimum at the 0° conformer and MP2 predicts a minimum at the 45° conformer, the energy difference between these two conformers is only about 0.1 kcal/mol .

The P–H stretching frequency is calculated too low by MM3 (-114 cm^{-1}) but is a frequency not modeled well by MM3. For each sp^3 oxygen attached to phosphorus, the P–H bond length is adjusted by an electronegativity correction. In theory, a force constant (k_s) electronegativity correction should also be applied. This correction has been determined for the specific case of C–H bonds but has not been resolved for P–H bonds.³³ As a consequence of the electronegativity of the adjacent sp^3 oxygens, the P–H bonds should be shortened and strengthened. Currently, MM3 is able to account for this shortening but not the strengthening of the bond.

P–H wagging frequencies calculated by MM3 and affected by the O=P–H, O–P–H, and H–P–H bending and the P=O stretching parameters differ from the scaled RHF frequencies by $+51$ and -57 cm^{-1} . The torsional modes, like those of hypophosphorous acid, also exhibit significant deviations. Once again, these discrepancies are the result of compromises made in fitting the overall data set.

Phosphoric Acid. Although X-ray and neutron diffraction studies have been performed for phosphoric acid, crystal-packing forces and intermolecular hydrogen bonding may be presumed to distort the structure. Additionally, the atomic position determined by analysis of X-ray data is the position of the center of maximum electron density, not the nuclear position. The P=O bond length is reported by X-ray and neutron diffraction to be 1.517 and 1.507 \AA , respectively, which is considerably longer than the scaled RHF/6-31G** result of 1.464 \AA . The neutron diffraction value is the distance between nuclei. The X-ray value is between centers of electron density and is longer than the neutron diffraction bond lengths due to the density associated with oxygen lone pairs. Similarly, the P–O X-ray and neutron diffraction bond lengths (approximately 1.57 and 1.56 \AA , respectively) are shorter than the corrected ab initio result of 1.584 \AA . Intermolecular hydrogen bonding may cause the P=O bond to lengthen and P–O bonds to shorten. Thus, comparisons of the gas-phase MM3 results with these solid-phase results are dubious, so our comparisons of structure focused on MM3 and scaled RHF results.

(42) Supporting Information available from the authors or the Internet.

Table 8. Phosphine Oxide^a

	IR ^b	RHF/6-31G**	scaled ^c	MM3	Δ IR ^d	Δ RHF ^e
P–H symmetric stretch	2359	2644	2380	2380	21	0
P–H asymmetric stretch	2371	2616	2354	2380	9	26
	2371	2615	2354	2367	–4	13
H–P–H symmetric bending	1240	1389	1251	1256	16	5
P=O stretching	1143	1282	1154	1127	–16	–27
H–P–H asymmetric bending	1114	1238	1114	1122	8	8
	1114	1238	1114	1122	13	13
H–P=O asymmetric bending	853	956	861	826	–27	–35
	853	956	861	826	–27	–35
rms					18	22

^a All vibrational frequencies in this table are expressed in cm^{-1} . ^b Experimental gas-phase IR is taken from: Withnall, R.; Andrews, L. *J. Phys. Chem.* **1987**, *91*, 784. ^c RHF/6-31G** vibrational frequencies are scaled by 0.90. ^d Difference between MM3 and experimental IR frequencies. ^e Difference between MM3 and RHF/6-31G** frequencies scaled by 0.90.

Table 9. Hypophosphorous Acid^a

	RHF/6-31G**	scaled ^b	MP2/6-31G**	scaled ^c	MM3	Δ RHF	Δ MP2
O–H stretching	4157	3742	3889	3694	3734	–8	40
P–H symmetric stretching	2690	2421	2610	2480	2388	–33	–92
P–H asymmetric stretching	2671	2404	2562	2434	2378	–27	–56
P=O stretching	1408	1268	1328	1261	1274	6	13
PH ₂ bending	1297	1167	1213	1152	1126	–41	–26
H–P–O symmetric bending	1243	1119	1163	1104	1095	–24	–9
P–O–H bending	1071	964	1048	996	965	1	–31
PH ₂ scissoring	990	891	934	888	937	46	50
P–O stretching	959	863	879	835	864	1	30
PH ₂ rocking	911	820	812	772	658	–162	–114
O=P–O bending	408	368	421	400	428	60	28
O–H torsion	86	78	234	222	261	183	39
rms						76	53

^a All vibrational frequencies in this table are expressed in cm^{-1} . ^b RHF/6-31G** vibrational frequencies are scaled by 0.90. ^c MP2/6-31G** vibrational frequencies are scaled by 0.95. ^d Difference between MM3 and RHF/6-31G**. ^e Difference between MM3 and MP2/6-31G**.

As in phosphorous acid, the O=P–O–H torsion is calculated by RHF/6-31G** to be less gauche (33.3°) than the MM3 calculated torsion (48.7°). As in previous cases, significant deviations between the ab initio and MM3 torsional frequencies exist, although the overall rms of 31 cm^{-1} for 19 frequencies is relatively good (Table S2). The RHF/6-31G* value for the O=P–O–H torsion can be accurately reproduced with the inclusion of a V_6 term to the MM3 torsional potential, and the O=P–O–H vibrational modes can be modeled better with the addition of a bend–torsion–bend term and the V_6 term to the force field.

Dimethylphosphinic Acid. The MM3 structure and frequencies of this molecule are in good agreement with the ab initio values, with an rms of 27 cm^{-1} for 30 frequencies (see Table S3). The inclusion of a torsion–stretch term to the potential further increases bond lengths of P–O bonds involved in eclipsed conformations.

Dimethyl Phosphonate. The two RHF O=P–O–CH₃ torsion angles in dimethylphosphonate are 29.9 and 50.6° , compared with corresponding MM3 values of 47.6 and 52.6° . As in phosphoric acid, the addition of a V_6 term would account for the difference in the former dihedral value. The RHF O=P–O angles are calculated as 114.1 and 117.6° , while MM3 calculates values of 115.0 and 115.4° . Likewise, the O–P–H angles are 105.0 and 99.9° , while MM3 determines a value of 101.9° for both. Torsion–bend cross terms would correct both of these discrepancies. The trans-lone-pair term allows the RHF P–O bond lengths (1.594 and 1.582 \AA) to be calculated reasonably close to the MM3 ones (1.594 and 1.583 \AA).

The solution IR modes determined by Nyquist were used for comparison with MM3 and are shown in Table

S4.³⁹ The largest difference in the frequencies (-178 cm^{-1}) is found for a PO₃ deformation mode. The RHF frequency for this mode is in better agreement ($+29 \text{ cm}^{-1}$) with experiment. Similarly, an MM3 C–O asymmetric bending frequency differs with experiment by -80 cm^{-1} and the RHF frequency by only -14 cm^{-1} . For reasons discussed previously, the MM3 P–H stretching frequency is 91 cm^{-1} lower than the experimental value.

Methyl Dimethylphosphinic Acid. Bond angle inconsistencies among the ab initio and MM3 structures also exist for this molecule. The RHF O=P–C angles are calculated to be 113.4 and 115.5° , while the MM3 results are 115.2° and 114.8° . The RHF O–P–C angles are calculated to be 100.8 and 104.6° compared to MM3 values of 102.3 and 103.1° . Again, inclusion of a torsion–bend term would reduce these differences. The vibrational frequencies in Table S5 are calculated well. The overall rms error is 26 cm^{-1} for 31 frequencies as compared with experiment and 27 cm^{-1} for 39 frequencies as compared with the RHF values.

Trimethylphosphine Oxide. An electron diffraction experiment was carried out by Wilkins and co-workers.⁴³ The MM3 structural results are within the limits of experimental error. The MM3 frequencies (Table S6) also agree well with the RHF calculated values, with the exception of a CH₃ in-plane wag frequency ($+109 \text{ cm}^{-1}$). The overall rms difference between MM3 and experiment is 31 cm^{-1} .

Trimethyl Phosphate. This structure is the only other one in the set with electron diffraction results.⁴⁴

(43) Wilkins, C. H.; Hagen, K.; Hedberg, L.; Shen, Q.; Hedberg, K. *J. Am. Chem. Soc.* **1975**, *97*, 6352.

(44) Oberhammer, H. *Z. Naturforsch* **1973**, *28a*, 1140.

Table 10. Conformational Distributions of 5,5-Dimethyl-2-substituted-2-oxo-1,3,2-dioxaphosphorinanes in Nonpolar Media^a

R	NMR % equatorial	ΔE^b (MM3)	MM3% equatorial	ΔE^c (MM3)	MM3% equatorial	RHF/6-31G** ^{b,f}
CH ₃ ^d	50–60	–5.3	100	–3.6	100	–3.7
OCH ₃	5–10	–0.7	76	–0.1	52	
H	10–20	–4.3	100	–2.9	99	
OH ^e	~50	–0.5	71	–0.2	57	

^a See ref 21. ^b ΔE = (equatorial – axial) energy difference in kcal/mol. ^c ΔE = (equatorial – axial) energy difference in kcal/mol for dielectric constant of 4.0. ^d See ref 48. ^e See ref 47. ^f MP2/6-31G**/RHF/6-31G** result is –3.6 kcal/mol.

The P–O bond length is calculated by MM3 to be 1.583 Å, which is in agreement with the experimental value of 1.580 Å. RHF angles were used instead of electron diffraction ones due to the large experimental deviations that exist because of error correlations. The minimum energy conformation was found by RHF calculations to have *C*₃ symmetry, with all O=P–O–Me torsions in a gauche orientation of 44.7°. The MM3 value for these torsion angles is 52.8°. As mentioned previously, if a *V*₆ torsional term could become part of the MM3 force field (in this case for the O–P–O–CH₃ torsion), the RHF result could be more accurately modeled.

Vibrational frequencies have been determined most recently in the aqueous phase by Burkhardt and co-workers.⁴¹ MM3 frequencies agree well with experiment, with the exception of a PO₃ and P–O–C bending mode. The overall rms errors for 14 experimental frequencies and 16 ab initio frequencies were 31 and 25 cm^{–1}, respectively (Table S7).

Dimethyl Methylphosphonate. This compound was not involved in the parametrization process but was used to validate the MM3 vibrational frequencies. The frequencies involving the phosphate atom type seem to agree well with the gas-phase IR results⁴⁵ as well as with the RHF/6-31G** ones (Table S8). The overall rms error is 27 cm^{–1} for 34 experimental frequencies and 27 cm^{–1} for 42 RHF vibrational frequencies.

2-Oxo-1,3,2-Dioxaphosphorinanes. To verify the parameters determined by modeling the nine phosphinic, phosphonic, phosphoric acids, and the related esters, conformational analysis of a series of substituted 1,3,2-dioxaphosphinane 2-oxides was performed with MM3, and the results were compared to available experimental NMR data. Conformational populations of 2-substituted-1,3,2-dioxaphosphinane 2-oxides can be determined by obtaining weighted time averages of the ³J_{PH} coupling constants, *J*_(POCH_A) and *J*_(POCH_B), where the methylene A and B protons are axial and equatorial, respectively, for compounds with axial substituents and vice versa (see Figure 9). One can indirectly calculate the ratio of conformers on the basis of the percentage of axial and equatorial methylene protons A and B that will fit the experimentally determined ³J_{PH} coupling constants. Some ratios of conformers shown in Figure 9 determined by this methodology are presented in Table 10.

White and co-workers concluded from their NMR study that methyl (as well as phenyl and benzyl) 2-substituted-1,3,2-dioxaphosphinane 2-oxides were “conformationally mobile on the nmr time scale,” and thus both conformations were present in solution. They also found that derivatives with an alkoxy (e.g. methoxy) or hydro (as well as halogeno) substituent exist “very largely as one conformer”, the axial one. The newly formulated MM3

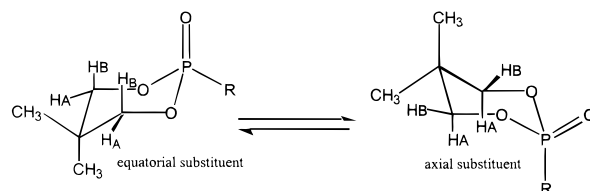


Figure 9. Axial and equatorial 5,5-dimethyl-2-R-oxo-1,3,2-dioxaphosphorinane. Conformational populations of these and similar compounds can be determined by obtaining weighted time averages of the ³J_{PH} coupling constants, *J*_(POCH_A) and *J*_(POCH_B), where the methylene A and B protons are axial and equatorial, respectively, for these compounds. One can indirectly calculate the ratio of conformers on the basis of the percentage of axial and equatorial methylene protons A and B that will fit the experimentally determined ³J_{PH} coupling constants.

force field predicts the methyl- and hydro-substituted compounds to be almost completely equatorial, while the methoxy-substituted conformers are predicted present to be in nearly equal amounts. Raising the dielectric constant to 4.0 (from the default value of 1.5) reduces some of the unfavorable dipole interactions in the axial conformers. However, increasing the dielectric constant does not account for the predominance of the equatorial conformation. The equatorial methyl-substituted compound is predicted by MM3 to be favored by 5.3 kcal/mol over the axial conformation resulting in 100% equatorial (3.6 kcal/mol with a dielectric constant of 4.0) compared to 50–60% equatorial determined by experiment.^{46,47} RHF/6-31G** calculations indicate that the equatorial conformer should predominate in the gas phase but by 1.6 kcal/mol less than MM3 determines this energy difference. Solvation may be responsible for at least part of the discrepancy between MM3 and the NMR experiments (phosphoric acid was used as a solvent in the 2-methyl-1,3,2-dioxaphosphinane 2-oxide experiment).⁴⁸ However, part of these energy discrepancies most likely occur because MM3 cannot reproduce very well the energetic consequences of an anomeric effect which has been measured in these compounds.

Generalized Anomeric Effect. The term “generalized anomeric effect” has been used to denote the preference of a conformer with a bond attached to an electronegative substituent (X) that lengthens if the lone pair on X is antiperiplanar to the bond (see Figure 10, where X is oxygen). This effect is well documented in the literature.^{25–27,29} A careful study of dimethoxymethane was undertaken by Kneisler,⁴⁹ and Cramer studied dihydroxy- and dimethoxymethane as well as 2-hydroxy

(46) Maryanoff, B. E.; Hutchins, R. O.; Maryanoff, C. A. *Top. Stereochem.* **1979**, *11*, 187.

(47) Donaldson, B.; Hall, L. D. *Can. J. Chem.* **1972**, *50*, 2111.

(48) White, D. W.; McEwen, G. K.; Bertrand, R. D.; Verkade, J. G. *J. Chem. Soc. (B)* **1971**, 1454–1461.

(45) Van der Veken, B. J.; Herman, M. A. *J. Mol. Struct.* **1983**, *96*, 233.

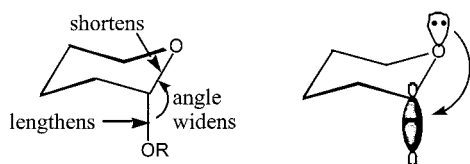


Figure 10. Anomeric effect for axial 2-hydroxy/alkoxytetrahydropyran ($R = H, CH_3$). In these systems, the C–O bond of the donor group shortens due to increased p character, the C–O bond of the acceptor group lengthens due to the ring oxygen lone pair orbital being antiperiplanar to the exo C–O antibonding orbital, and the O–C–O bond angle widens.

and 2-alkoxytetrahydropyran (sugar) systems.^{30,50} For these systems, the C–O bond of the donor group shortens due to increased p character, the C–O bond of the acceptor group lengthens due to the ring oxygen lone pair orbital being antiperiplanar to the exo C–O antibonding orbital, and the O–C–O bond angle widens (see Figure 10).

With NBO analysis, the role of hyperconjugation, specifically $n \rightarrow \sigma^*$ delocalization, has been demonstrated.^{26,27,30} Energetic stabilization of axial conformers has been quantitatively established with NBO by measuring the overall SCF energy E_{tot} , the energy due to bonding/covalent interactions E_{Lewis} , and the energy due to antibonding/noncovalent interactions E_{del} . Second-order perturbation analysis provides insight into specific orbital interactions, and thus one can identify those orbitals that largely contribute to the energy differences between conformers. For the case of 2-hydroxy- and 2-alkoxytetrahydropyran (Figure 10), $n_O \rightarrow \sigma_{C-O}^*$ stabilizes the axial conformer. For the case of 2-R-1,3,2-dioxaphosphinane 2-oxides ($R = CH_3, H,$ and OH) and other molecules where oxygen lone pairs are antiperiplanar to P–R bonds, the same $n_O \rightarrow \sigma_{P-R}^*$ orbital interaction is observed. In addition, for the equatorial conformer, the P=O bond is lengthened due to $n_O \rightarrow \sigma_{P=O}^*$.

The specific case of 2-methyl-1,3,2-dioxaphosphorinane oxides is illustrated in Table 5. Note that the P–CH₃ bond of the axial conformer is lengthened compared to the equatorial one, and the equatorial conformer's P=O bond is lengthened compared to the axial one. As mentioned in the Computational section, NBO analyses were undertaken at the RHF level with the 6-31G*, D95*, and cc-pVDZ basis sets. Both the 6-31G* and cc-pVDZ basis sets gave spurious energy results and a E_{del} of greater than 150 kcal/mol! Clearly, a problem exists when carrying out an NBO analysis using these basis sets, although the E_{tot} is reasonable compared to results obtained when using the other two basis sets. The D95* and cc-pVDZ results are presented in Table 11 (see Figure 11). Although the SCF energy of the equatorial conformer is lower than the axial by 3.9 kcal/mol, this energy analysis reveals that this energy discrepancy would be much greater if one only considered the Lewis energy. In fact, the axial conformer is stabilized by 6.4 kcal/mol of delocalization energy (see Table 11). Molecular mechanics can account for this effect with an appropriate bond torsion–stretch term for bond lengths and a torsion–bend term for bond angles. Unfortunately, MM3 does not possess such a torsion–bend term. How-

Table 11. Hartree–Fock Second-Order Perturbation NBO Deletion Energies for 2-Methyl-2-oxo-1,3,2-dioxaphosphorinane^a

X	Y	6-31G*			cc-pVDZ			D95*		
		E_{tot}	E_{Lewis}	E_{del}	E_{tot}	E_{Lewis}	E_{del}	E_{tot}	E_{Lewis}	E_{del}
CH ₂	CH ₂	0.6	1.3	0.7				0.8	2.3	1.5
O	CH ₂	3.3	4.9	1.3	3.2	6.8	3.6	3.3	7.0	4.3
O	O	3.9	150.2	146.3	3.9	147.2	143.3	3.9	10.3	6.4

^a All energies are the difference between the axial and equatorial conformations and are expressed in kcal/mol.

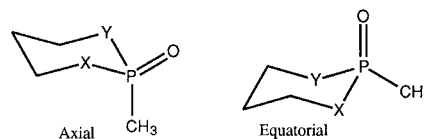


Figure 11. Axial/equatorial 2-methyl-1,3,2-dioxaphosphinane 2-oxide ($X = Y = O$) (10), axial/equatorial 2-methyl-1,2-dioxaphosphinane 2-oxide ($X = O, Y = CH_2$) (12), and 1-methylphosphorinane 1-oxide ($X = Y = CH_2$) (11).

ever, preliminary work with MM4, which includes this term, shows that bond angles and conformer energy differences can be reproduced in molecules exhibiting these effects. These results will be presented in later work.

Conclusions

RHF/6-31G** geometries, rotational barriers, dipole moments and vibrational frequencies for nine phosphinic, phosphonic, and phosphoric species were used to parameterize the MM3 force field. Comparisons of MM3 and experimental results were made when available. MM3 results are in good agreement with most of the experimental results. Some of the MM3 optimized O=P–O–X torsions for these compounds vary from the RHF/6-31G** values by approximately 15° due to a shallow well in the 0–60° region. Negative hyperconjugation has been observed for bonds with one or more sp³ oxygens attached to phosphorus. The Bohlman (trans lone pair) correction term in MM3 is able to account for this effect. Discrepancies between MM3 and ab initio results exist for 2-substituted-1,3,2-dioxaphosphinane 2-oxides due to the inability of MM3 to account for the energetic consequences an anomeric effect in conformers with an axial substituent. An even larger energy difference between MM3 and experiment more than likely results from solvent stabilizing the more polar axial conformer. Thus, MM3 calculates the equatorial conformer to be more stable than the axial one. Increasing the dielectric constant in MM3 stabilizes the axial conformations, which is expected since the axial conformers have larger dipole moments. NMR experiments show that an equilibrium exists, often favoring the axial conformer.

Acknowledgment. We thank Triplos, Inc. for their support of this work.

Supporting Information Available: Tables of experimental, ab initio calculated, and MM3 calculated IR frequencies for oxygen-containing phosphates (12 pages). This material is contained in libraries on microfiche, immediately follows this article in the microfilm version of the journal, and can be ordered from the ACS; see any current masthead page for ordering information.

(49) Kneisler, J. R.; Alliner, N. L. *J. Comput. Chem.* **1996**, *17*, 757.
 (50) Cramer, C. J.; Truhlar, D. G.; French, A. D. *Carbohydr. Res.* **1997**, *298*, 1–14.